SoilChip-XPS integrated technique to study formation of soil biogeochemical interfaces

Xizhi Huang [a, b], Yiwei Li [c], Bifeng Liu [c], Georg Guggenberger [a, d], Olga Shibistova [d, e], Zhenke Zhu [a], Tida Ge [a, **], Wenfeng Tan [f], Jinshui Wu [a, *]

[a] Key Laboratory of Agro-ecological Processes in the Subtropical Region, Institute of Subtropical Agriculture, The Chinese Academy of Sciences, Changsha 410125, China
[b] University of Chinese Academy of Sciences, Beijing 100049, China
[c] Britton Chance Center for Biomedical Photonics at Wuhan National Laboratory for Optoelectronics − Hubei Bioinformatics & Molecular Imaging Key Laboratory, Systems Biology Theme, Department of Biomedical Engineering, College of Life Science and Technology, Huazhong University of Science and Technology, Wuhan, PR China
[d] Institute of Soil Science, Leibniz Universität Hannover, 30419 Hannover, Germany
[e] VN Sukachev Institute of Forest, Russian Academy of Sciences - Siberian Branch, Akademgorodok, 660036 Krasnoyarsk, Russia
[f] Key Laboratory of Arable Land Conservation (Middle and Lower Reaches of Yangtze River), Ministry of Agriculture, College of Resources and Environment, Huazhong Agricultural University, Wuhan 430070, China

ARTICLE INFO

ABSTRACT

Many soil functions are modulated by processes at soil biogeochemical interfaces (BGIs). However, characterizing the elemental dynamics at BGIs is hampered by the heterogeneity of soil microenvironments. In order to investigate the processes of BGI formation in an upland soil (Mollisol) and a paddy soil (Oxisol), we developed a SoilChip method by assembling dispersed soil particles onto homogeneous 800-μm-diameter microarray chips and then submerging them in a solution that contained dissolved organic matter (OM) extracted from one of the two soils. The chips with Mollisol particles were incubated at 95 −100% humidity, whereas the chips with Oxisol particles were incubated at 100% humidity. Dynamics of individual elements at the soils' BGIs were quantitatively determined using X-ray photoelectron spectroscopy (XPS). Distinct differences in the soil-microbe complexes and elemental dynamics between the Mollisol and Oxisol BGIs suggested that the formation of specific BGIs resulted from the complex interaction of physical, chemical, and microbial processes. By integrating the SoilChip and XPS, it was possible to elucidate the dynamic formation of the two different soil BGIs under standardized conditions. Therefore, the SoilChip method is a promising tool for investigating micro-ecological processes in soil.

© 2017 Published by Elsevier Ltd.

1. Introduction

Soil biogeochemical interfaces (BGI) within the three-dimensional soil structure are considered unique and represent complex hotspots of microbe-soil interactions (McClain et al., 2003; Chorover et al., 2007; Totsche et al., 2010). The formation of BGIs can alter the physical-chemical properties of soil, such as its wettability, for which changes can result in the formation of preferential water flow, thus affecting the transport and fate of dissolved compounds, clay minerals, and microorganisms (Goebel et al., 2011). Furthermore, in addition to the association of microbes with the BGIs of primary and secondary particles, microbes also transform and decompose organic matter (OM) and secrete extracellular polymeric substances (EPS) to modify their environment (Gleixner, 2013; Kleber et al., 2015).

The chemical extraction methods that have traditionally been used to investigate the biogeochemical behavior of elements obscure the details of microbe-soil interactions (Lehmann and Kleber, 2015). Furthermore, soil fractionation techniques, which are based on the operational separation procedures for bulk soil samples, will also homogenized the microenvironment of the

---

* Corresponding author. Institute of Subtropical Agriculture Chinese Academy of Sciences, No. 644, Mapoling of Changsha City, Hunan Province, PR China.
** Corresponding author. Institute of Subtropical Agriculture Chinese Academy of Sciences, No. 644, Mapoling of Changsha City, Hunan Province, PR China.
E-mail addresses: huang.xizhi@163.com (X. Huang), gtd@isa.ac.cn (T. Ge), jswu@isa.ac.cn (J. Wu).

microbial habitat, and are not suited to investigate the linkages between habitat architecture and biological functioning (Six et al., 2004; Young and Crawford, 2004). Recently, advances in non-destructive techniques for soil microaggregate analysis have enriched our understanding of elemental cycling traits in soil at the microscale (Wan et al., 2007; Remusat et al., 2012). For example, the use of nanoscale secondary ion mass spectrometry (NanoSIMS) revealed that fresh OM preferentially attaches to partially rough surfaces (Vogel et al., 2014). Lehmann et al. (2008) used near-edge X-ray fine structure spectroscopy (NEXAFS) to illustrate that the nanoscale carbon species distribution of OM exhibited significant heterogeneity at specific mineral surfaces. However, most soil surface characteristics are investigated using one-time snapshot measurements, which are of limited use for assessing the dynamic mechanisms of multi-element cycling and microbe-mediated transformations at the microsite scale (Lützow et al., 2006; Lehmann and Kleber, 2015). Thus, mineral-OM-microbe interactions at the soil BGI are still poorly understood (Huang et al., 2005; Chorover et al., 2007; Totsche et al., 2010; Mueller et al., 2013; Sparks, 2015). There is growing concern regarding the importance of microscale and dynamic processes at the soil BGI, which could unravel the linkage between physical-chemical and biological processes within the continuum of soil-microbe interactions (O'Donnell et al., 2007; Kuzyakov et al., 2009; Remusat et al., 2012).

The development of "lab on a chip" techniques, such as microfluidics and microfabrication, has facilitated the microscale confinement of small objects, such as bacterial populations and cells, and has provided powerful tools for exploring microscale and dynamic processes (Weibel et al., 2007; Wessel et al., 2013). For example, Kim et al. (2008) used microfluidics to co-culture microbes and clearly demonstrated that a proper spatial distribution stabilized multi-species bacterial communities. In addition, Valiei et al. (2012) used microfluidic porous media mimics, in which an array of polydimethylsiloxane (PDMS) microposts were embedded in a microchannel, to monitor the behavior of microbe transportation in a soil pore system and found that hydrodynamics govern the formation, morphology, and distribution of biofilm streamers. Moreover, novel devices such as the RootChip and PlantChip, which take advantage of miniaturization for handling small volumes of liquids, have been developed for plant cell analysis, thus facilitating large-scale investigations of root metabolism and signaling (Grossmann et al., 2011). These applications suggest that "lab on a chip" techniques could also be useful for mimicking soil processes.

Inspired by the complex and adaptive nature of soils, in which mineral particles, OM, and microbes self-organize into complex aggregates, and the structural dynamic evolves with changing microenvironments (e.g., available C, nutrients, or water; Oades and Waters, 1991; Young and Crawford, 2004; Jozefaciuk and Czachor, 2014), we applied a controllable microfluidic method to reconstruct a soil suspension, in which all the bulk soil components were included, onto homogeneous microarray chips, which were then submerged in dissolved organic matter (DOM) to initiate soil BGI processes. For the tracking of multi-element dynamics at the soil surface, the SoilChip was coupled with X-ray photoelectron spectroscopy (XPS), a sensitive surface detecting method with a penetrating depth of $<5–10$ nm, which is perfectly suited for investigating mineral surfaces (Amelung et al., 2002; Woche et al., 2017). We tracked temporal dynamics of the BGI formation and modification through the different sampling time during the 21-d incubation and followed by XPS measurements.

Our objective was to develop a SoilChip method to mimic a soil microenvironment that could be used to assess the heterogeneous and temporally dynamic properties of microinterfaces. By comparing two different soils, a Mollisol and an Oxisol, we aimed to elucidate the effects of different interface and solute compositions on BGI formation.

2. Materials and methods

2.1. Soil sample characterization

Two contrasting soil samples were used for our experiments: a Mollisol from a long-term fertilization trial at Gongzhuling, Jilin Province, China, and an Oxisol from a continuous (>30 years) rice plantation at the Taoyuan Station of Agro-ecology Research in Hunan. The top layer ($0–20$ cm depth) of both soils was sampled, air dried in the laboratory for one week, gently crushed with a wood rolling pin, and then passed through a 2-mm sieve. Visible organic residues were then removed from the samples using forceps, after which the physicochemical properties of the soil samples were determined using standard procedures (Li et al., 2008; Chen et al., 2012; Table S1).

2.2. Soil suspension preparation and DOM extraction

The two soils were pre-incubated in the dark for one week at 45% water holding capacity and a constant temperature of 25 °C, in order to allow the microorganisms to recover to their normal activity levels. After pre-incubation, each soil was divided into three parts, for 1) assembly of soil microaggregates on the SoilChip, 2) DOM extraction, and 3) micro interface analysis of the soil aggregate. Fresh field soil (1 g d.w. equivalent) was vortexed (800 r min^{-1}) in 3 ml distilled water for 2 min, sonicated at 60 W min^{-1} for 3 min (Biosafer1000; Biosafer, Nanjing, China) to disperse soil macroaggregates, and passed through a <0.25-mm sieve to remove particulate OM. The particle size distribution of the suspensions was determined using a Mastersizer 3000 (Malvern Instruments, Worcestershire, UK). To strengthen the structure of the microaggregates assembled on the SoilChip, polyvinyl alcohol (PVA) was added to the soil suspensions (500:1 mass ratio of PVA and soil) to act as an organic cement (Cai et al., 2013).

To construct the soil microenvironment, DOM solutions were extracted from the two incubated soils and used to cover the soil microarrays. The solutions were prepared by mixing fresh soil (1 g d.w. equivalent) with double distilled H$_2$O at a soil:water ratio of 1:2 (volume:mass), sonicating the samples at 120 W min^{-1} for 3 min, obtaining supernatants by centrifugation at 8800 × g for 4 min, and pressure filtering the supernatants through 0.2-μm polysulfone membranes (Whatman, Inc., Springfield Mill, UK) to remove microbial bio- and necromass and clay particles. The organic carbon (OC) concentrations of the DOM solutions were measured using a TOC-5050A total organic C analyzer (Shimadzu, Kyoto, Japan).

2.3. SoilChip construction

To obtain a controllable and uniform soil interface, microfluidic devices with hydrophilic microarrays for depositing the soil particles were produced using oxygen plasma modification (Li et al., 2016). Briefly, a stamp of PDMS with 800 μm-diameter cylindrical wells was produced using standard soft lithography methods (Fig. 1a; Weibel et al., 2007). Then, the PDMS stamp and a clean glass slide were modified into super hydrophilic interfaces using low-oxygen plasma exposure treatment for 1 min (PDC-GC-M; Weike Spectrum Instrumental Technology Development Co., Ltd., Chengdu, China). Thereafter, the PMDS was quickly sealed to the glass and torn off. Areas of the glass that were coated with PDMS film became hydrophobic, whereas those without PDMS remained
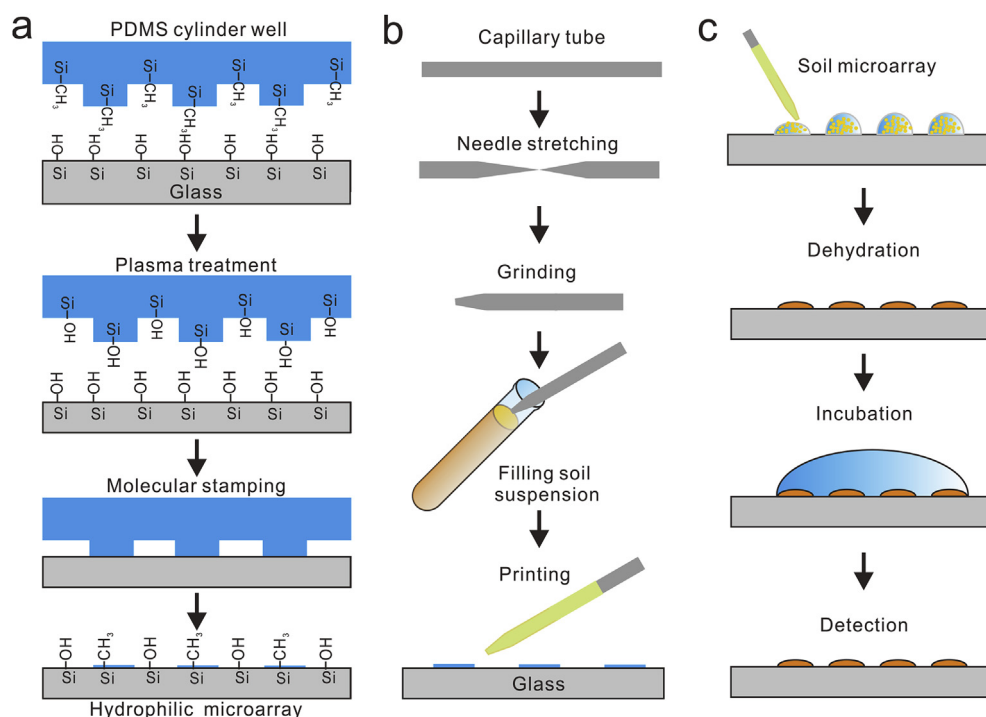
Fig. 1. SoilChip setup. a) A polydimethylsiloxane (PDMS) stamp with 800 μm-diameter cylindrical wells was produced using standard soft lithography, and the clean glass and PDMS stamp were treated using oxygen plasma modification. Afterward, the PDMS stamp was printed on the glass and quickly removed by hand, resulting in the formation of a hydrophilic microarray. b) A capillary needle was produced using a stretching machine, and the needle was ground to provide an opening of 300–500 μm. Then, using capillary force, the needle was filled with the soil suspension. c) Printing occurred as the needle contacted the hydrophilic areas. After the water evaporated, the soil microarray was covered with dissolved organic matter from the same soil, resulting in a fully constructed SoilChip. Subsequently, the SoilChip was incubated under constant moisture and dark conditions. For surface analysis, the dissolved organic matter was removed from the SoilChip by gravity force, and the soil was air-dried for measurement.

hydrophilic and served as the microarrays for the soil suspension. Although areas of PDMS were introduced in the soil microenvironment, previous studies have shown that PDMS, a kind of non-polar and biocompatible material, does not sorb much polar DOM (Sapsford and Ligler, 2004). Hence, DOM sorbed on the soil dots should represent the total DOM. Further, no toxicity is reported for microbial deposition and growth (Weibel et al., 2007). Thus, we consider that the limited area of PDMS film did not alter soil conditions, thereby impacting processes associated with BGI formation.

For printing (Fig. 1b), a borosilicate glass capillary (OD: 1.0 mm, ID: 0.78 mm, length: 10 cm; Sutter Instrument Company, Novato, CA, USA) was manufactured into a needle using a needle puller (PN - 30; Narishige, Tokyo, Japan). The tip was ground to a diameter of 300–500 μm so that the soil suspension could easily flow out when the needle came in contact with the array's hydrophilic areas. The soil suspension flowed into the glass capillary needle by capillary force, and afterward, droplets were printed across the glass substrate to form microarrays. As the water evaporated, the soil microparticle arrays self-assembled at the defined hydrophilic sites, resulting in 8 × 8 soil microarrays (single dot size: 800 μm diameter and ~50 μm height). Finally, the soil microarrays for each soil type were covered with 0.15 ml DOM solution that was extracted from the same respective soil (Fig. 1c), and were put into a Petri dishes with water.

Subsequently, the SoilChip setup was incubated for 21 d in a dark container at 25 °C. Since the land use of the two soils was different, the Mollisol and Oxisol chips were incubated at different levels of humidity. The Oxisol chips were incubated at 100% relative humidity, conditions under which our preliminary experiments indicated that no significant amount of water was lost from the SoilChip, whereas the Mollisol chips were incubated under dynamic humidity conditions (~95–100%) at 25 °C and in a container with a fan, conditions under which half of water gradually evaporated from the SoilChips during the 21-d incubation.

Since microinterface changes can occur rapidly at the beginning of such incubations, we sampled more intensively at the start of the experiment and at longer time intervals thereafter. During sampling, the excess DOM solution on the SoilChip was removed by gravity, and the thin film of water that remained mimicked the soil's natural field capacity. Thereafter, the microarray samples were air-dried at 45 °C for 30 min in preparation for direct surface analysis.

2.4. Surface characterization

We used scanning electron microscopy (SEM; Nova NanoSEM50, FEI, Netherlands) to analyze the morphology of the assembled surfaces and microbes, and microbial cells were distinguished using both morphology and the detection of C concentration by energy dispersive X-ray spectroscopy (EDX; New XL-30; Philips, Mahwah, NJ, USA; Kaiser et al., 2002).

For XPS measurement, air-dried soil aggregates and freeze-dried DOM were fixed using the traditional double-sided adhesive tape method. To eliminate the effect of the microarrays' heterogeneity on the XPS measurements, a 300 × 500-μm area of each dot was randomly chosen and analyzed using an AXIS-ULTRA DLD-600W apparatus (Kratos, Manchester, UK), as described previously (Mikutta et al., 2009). Briefly, wide-scan spectra with a 0.4 eV step, covering a binding energy (B.E.) range from 0 to 1250 eV, were obtained, and mass ratios of Al, Fe, C, O, N, Na, Mg, Ca, and Si were calculated from the areas of the Al 2p, Fe 2p, C 1s, O 1s, N 1s, Na (KLL
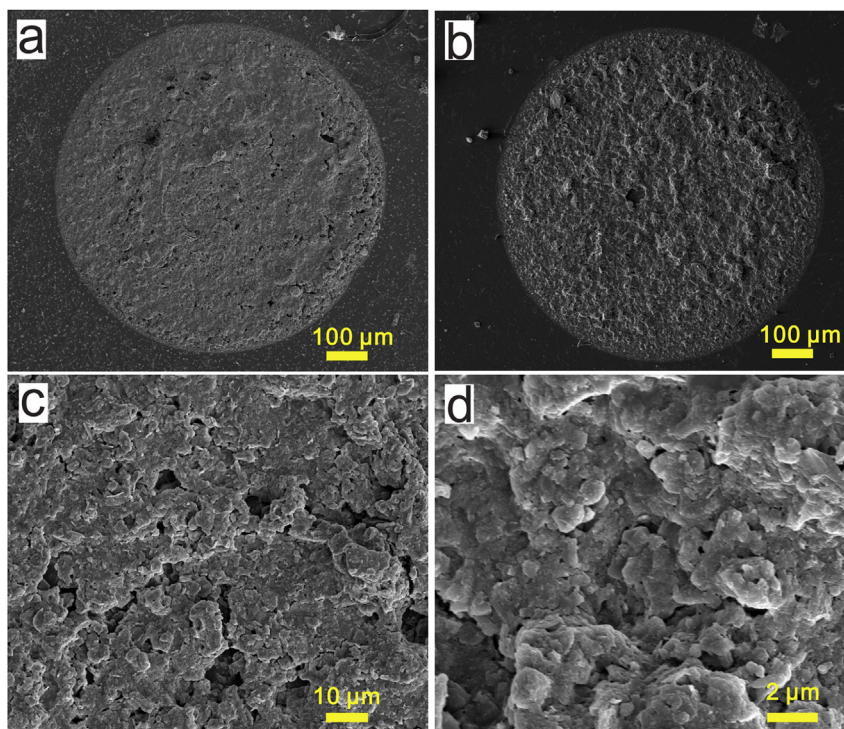
Fig. 2. Homogeneous morphology of soil surfaces on the SoilChip. (a) and (b) Scanning electron microscopy (SEM) images of two replications of self-organized soil particles on the SoilChip, with 100-μm scale bars. (c) and (d) Details from (a) with 10- and 2-μm scale bars, respectively.

Auger), Mg (KLL Auger), and Si 2s peaks, respectively, using experimentally determined atomic sensitivity factors. Sample charging during analysis was corrected based on the maximum principal ^{C1}s sub-peak centered at 284.8 eV. In addition, the Si 2p/Si 2s ratio for the eight soil microarray samples was used to verify the method's accuracy; the ratio ranged from 0.97 to 1.03 (1.00 ± 0.02, n = 8), which was within acceptable limits (Yuan et al., 1998). To analyze the chemical state of the C and N, narrow-scan spectra of C1s and N1s with a 0.05 eV step were obtained. The survey and narrow-scan XPS analyses of soil surfaces on the SoilChips in different periods of incubation were carried out in duplicate or triplicate.

3. Results

3.1. Homogeneous and durable soil microinterface production

The size distribution of the soil particles, which were <50 μm in diameter (Fig. S1), indicated that the combination of vortexing and ultrasound treatment was an efficient method for obtaining homogeneous soil suspensions. After the soil suspensions were assembled into microarrays on the chips, the surface of the Oxisol chip was analyzed, as an example. The resulting SEM images indicated that each soil dot on the Oxisol SoilChip possessed homogeneous surface morphology and rim shape (Fig. 2a and b). The area around the soil dots (Fig. 2a and b) represented the PDMS-coated region. Owing to the self-assembly of the soil suspensions, microscale heterogeneity (e.g., concerning pores <30 μm) was still observed within each soil dot (Fig. 2c and d), which was consistent with the soil particle size distribution (Fig. S1). The morphology of the Mollisol dots on the soilchip is as similar as the Oxisol. To reduce the small-scale variability of elements at the soil microsurfaces, a 300 × 500-μm area, was randomly selected for XPS measurement.

No significant (p < 0.001) changes were observed in the concentrations of elements at the BGIs with the addition of <0.2% PVA (Table S3), and the chemical states of both C and N also remained unchanged (Fig. S3), which is consistent with previous reports (Cai et al., 2013). However, the addition of PVA significantly enhanced the mechanical stability of the soil microarray, which allowed the SoilChip to be incubated for more than one month without being destroyed by the surface tension associated with dehydration.

3.2. Reliable use of the SoilChips for XPS analysis

At the newly assembled soil surfaces, almost all elements with relative mass concentrations of >0.5% exhibited relative standard deviations (RSD) of <10% at the XPS measurements for both soil types (Table 1), which is consistent with previous reports that the accuracy of XPS quantitative analysis can reach 10% (Arnarson and Keil, 2001; Yuan et al., 1998). Elements with concentrations below 0.5%, such as P and S in the Mollisol and P and Ca in the Oxisol (Table 1), possessed greater variation, and in the Oxisol, the RSD for Al was relatively large (13%), despite having a concentration of 10%. Accordingly, heterogeneity in element concentration arose from both analytical error and heterogeneity in the element distribution on the micro-array. However, according to previous studies (Arnarson and Keil, 2001; Yuan et al., 1998), a RSD of elements for XPS measurement <14% is acceptable, thus indicating a quite good elemental homogeneity of the soil dots in the present study. The heterogeneity of the OM composition on the soil microarrays was assessed according to the C and N binding states. Four C species of C 1s were quantified at the SoilChip surface (Fig. S2a, b and c) and were attributed to aliphatic carbon (C-H and C-C; 284.8 eV and 285.5 eV), alcohol carbon (C-O and C-N; 286.5 eV), amide carbon (O=C-N; 288 eV), and carboxylic carbon (O=C-O-; 289.3 eV; Chastain et al., 1995). Comparison of the high-resolution C 1s spectra of three replications indicated that every new surface

Table 1
The elemental composition of SoilChip surfaces before incubation.[a]

Elements (%)	C	N	Fe	S	Mg	Si	Al	P	K	O	Ca
Mollisol	22.2	0.4	1.3	0.4	0.3	33.0	8.0	0.4	0.4	32.4	0.8
	21.4	0.3	1.6	0.2	0.3	31.7	7.7	0.0	0.4	34.6	1.0
	20.8	0.3	1.3	0.2	0.5	32.3	8.9	0.3	0.3	33.6	1.1
Mean values	21.5	0.4	1.4	0.3	0.3	32.3	8.2	0.2	0.4	33.5	1.0
RSD (%)	2.7	8.4	8.5	38.5	23.9	1.6	6.4	70.9	13.2	2.7	11.3
Oxisol	19.6	0.3	1.1	0.4	0.1	32.8	11.7	0.3	0.2	33.3	0.3
	19.8	0.4	1.0	0.3	0.2	32.9	9.9	0.2	0.3	34.7	0.3
	23.2	0.3	1.3	0.4	0.2	34.6	8.5	0.1	0.4	30.8	0.2
Mean values	20.9	0.4	1.1	0.4	0.2	33.4	10.0	0.2	0.3	32.9	0.3
RSD (%)[*]	8.0	9.6	11.2	8.8	19.7	2.5	13.0	45.5	17.6	5.0	15.0

[a] Assessed by X-ray photoelectron spectroscopy. RSD: relative standard deviation (n = 3).

assembled on the SoilChip possessed similar chemical properties (Table S2). This is also supported by the N 1s spectra (Fig. S2d, e and f), where similar peaks at 400.2 eV (amine/amide N and protonated amines) and at 401–402 eV (quaternary N) were observed on the triple Oxisol surfaces (Chastain et al., 1995).

The reliability of the SoilChip method for quantifying elemental dynamics during BGI formation was verified on the Oxisol surface. The RSD of almost all elements (C, N, Fe, S, Mg, Si, Al, P, K, O, and Ca) were used to assess the heterogeneity of elements at the BGI during the 21-d incubation. The RSD values of most of the main elements (concentration >0.5%) were <15% (black dashed line; Fig. 3), a level considered acceptable for the continuous tracking of element dynamics at the BGI.

3.3. Undisturbed soil-microbe complex on the SoilChip

After 13 d of incubation, stick-like objects of different sizes emerged at the soil surfaces (Fig. 4a and c), and energy dispersive X-ray spectroscopy (EDX) revealed that the objects on the Mollisol surface (e.g., site 1 in Fig. 4a) had a higher mass ratio of C/Si (57.8%/ 7.1%) than the adjacent surfaces (e.g., site 2 in Fig. 4a and b; 9.1%/ 20.3%). Therefore, it was reasonable to assume that these features represented microbial biomass or necromass. Soil-microbe complexes formed during the incubation, as well, and the progression of microbial activity on the SoilChip was reflected by the temporal development of the C/N ratios (Fig. 4d). In the Mollisol, the C/N ratio decreased sharply after the start of the incubation, so that, after 3 d, the C/N ratio of the Mollisol BGI had declined from 65 to 7.7, which is close to the bulk soil's C/N ratio of 8.4 (Table S1). However, after the 21-d incubation, the C/N ratio gradually increased again to 19. In contrast, the Oxisol exhibited a much slower reduction in the C/N ratio, decreasing from 59.4 to 20.0 after 3 d of incubation and to 16.3 after 21 d.

3.4. Dynamics of elemental interactions at the BGIs

At the BGIs of both soil types, the elemental dynamics indicated that inorganic surfaces, represented by Si and Al, decreased with incubation time, whereas C and N increased, as a result of the accumulation of OM (Fig. 5a–d). However, the extent of the organic and inorganic interaction during the BGI formation of the two soils was markedly different. For the Mollisol, Si declined from 32 to 6.3%, and Al and Fe nearly disappeared after 21 d of incubation, whereas C continuously increased to 51% (Fig. 5a and b). In contrast, for the Oxisol Si and Al together decreased by 12.5%, whereas Fe remained unchanged, and C increased to only 26.2%. In addition, after 21 d of incubation, N at the BGIs of the Mollisol and Oxisol reached concentrations of 2.8 and 1.9%, respectively (Fig. 5e and f),

which clearly indicated that the BGIs of both soils were enriched in N, as compared to the content of bulk soils (Table S1) and the original aggregate surfaces (Table S4). During incubation, the Ca concentration at the Mollisol BGI was enriched from 0.8% to 2.4%, whereas the Ca concentration at the Oxisol BGI remained unchanged <0.3% (Fig. 5e and f). This observation is related to the much higher contents of exchangeable Ca in the Mollisol (Table S1), which implies that the two soils also underwent contrasting pedogenetic development processes.

4. Discussion

In the present study, we tested whether a "Lab on a Chip" approach is useful for studying soil processes. We first investigated whether the principle approach is feasible, by providing stable and relatively homogenous surfaces that can be used in incubation experiments, and then used the method to investigate the formation processes of BGIs in two different soil types.

4.1. Soil microenvironment construction

The soil surface on the SoilChips possessed acceptable homogeneity with respect to morphology (Fig. 2), element concentrations (Table 1), and the chemical state of C 1s and N 1s (Fig. S2; Table S2). Thus, the self-assembly of dispersed soil on the
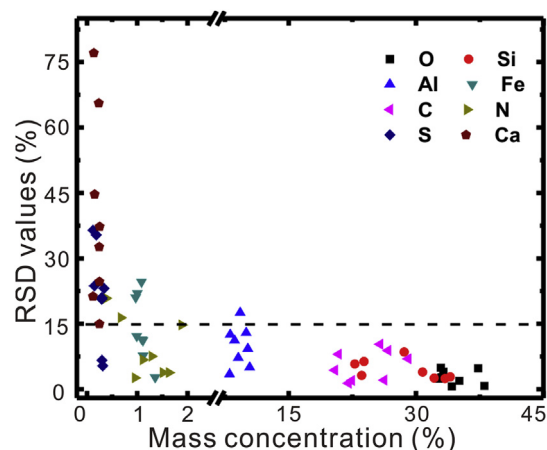
Fig. 3. Variation in the element contents at the soil biogeochemical interface during the 21-d incubation of the Oxisol as determined by X-ray photoelectron spectroscopy. Red dashed line indicates 15% relative standard deviation. (For interpretation of the references to colour in this figure legend, the reader is referred to the web version of this article.)
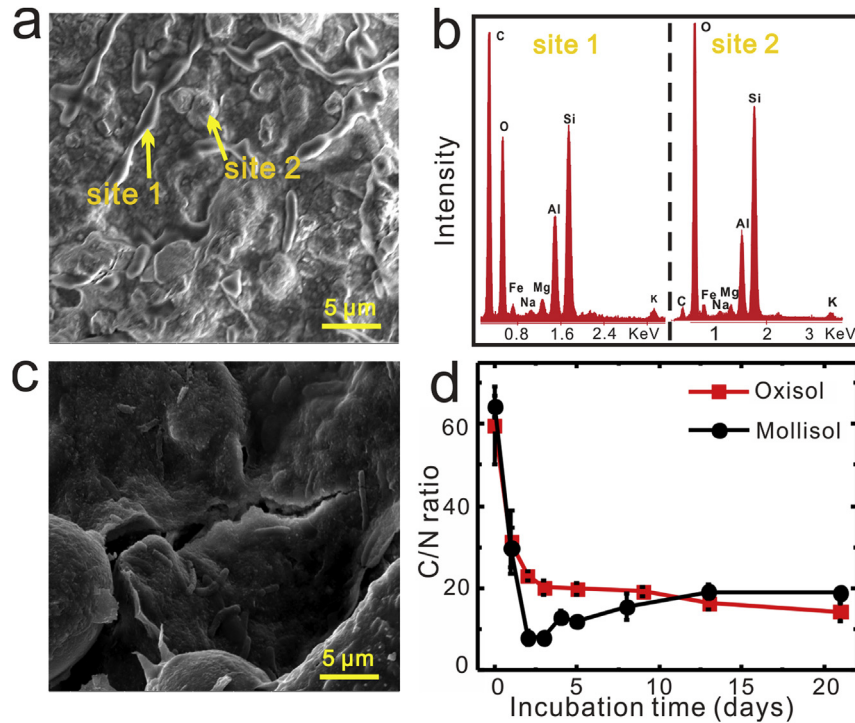
Fig. 4. Formation of the soil-microbe complex on the SoilChip. (a) and (c) SEM images of the Mollisol and Oxisol biogeochemical interfaces, respectively, after incubation of 13 d. (b) Energy-dispersive X-ray spectroscopy data, confirming much higher carbon contents of the microbial biomass at the interface (site 1) than in soil particles without microbes (site 2). (d) The development of the C/N ratio of the biogeochemical interfaces over the course of the incubation also indicated microbial processes. The error bar calculated by three samples measurement, except some point of Mollisol samples with two replicated measurements.

hydrophilic microarrays is an excellent method to produce quite homogeneous and stable soil microsurfaces.

The RSD of element contents varied between 1.6% and 13% for major elements (mass concentration >0.5%; Table 1), of which about 10% can be attributed to the analytical error of XPS measurements (Yuan et al., 1998), and, consequently, only a minor part of the variation was due to the not completely homogenous element distribution on the soil surface. The relative larger heterogeneity of Al in the Oxisol compared to the Mollisol (Table 1) was likely due to a not entirely complete soil dispersion and a less homogeneous sorption of dissolved Al on soil surfaces. The Oxisol had a much larger Al concentration in solution due to the low pH (Table S1). Along with the DOM, Al was sorbed to, or precipitated on, Oxisol surfaces after dehydration on SoilChip, thus probably accentuating the inherent heterogeneity, which was likely caused by the larger particle size (Fig. S1). In addition, the formation of spots of OM on the soil surface could have contributed to some heterogeneity of the chemical composition of the soil surfaces, as was indicated by an uneven distribution of fluorescently labeled organic substance in soil dots during the dehydration. Nevertheless, we consider the variability of major elements as acceptable, as it can be related to the inherent heterogeneity of the samples at the scale of observation.

Our data indicated that the OC contents at the aggregate surface of the original Mollisol and Oxisol (Table S4) were 5.3- and 6.3-fold greater, respectively, than those in the bulk soil (Table S1). This is consistent with previous reports that OM tends to concentrate at the soil aggregate surface (Amelung et al., 2002). At the newly formed soil microsurface on the SoilChip, we observed that OC accumulated to levels of up to 20.9% in the Oxisol and up to 21.5% in the Mollisol (Table 1). Since there was no significant effect of PVA on C enrichment (Table S3), this increase could be attributed to the self-assembly processes of the soil suspension. During the

evaporation of water after printing, the OM probably concentrated in the solution and precipitated onto newly exposed active mineral surfaces, contributing to the high OC content at the surface. This process may have been supported by the decrease of Fe, Al, and O at the newly assembled surface on the SoilChip (Table 1), as compared to the aggregate surface composition of the original soil (Table S4). Accordingly, our soil microarray investigation demonstrated that the evaporative self-assembly of the fine particles could redistribute and concentrate the soil OM at the surface of the soil dots, which probably provides a clue for understanding the formation of OM hotspots in soil (Vogel et al., 2014).

Artificial soil experiments have been used successfully to improve our mechanistic understanding of soil functions. For example, Pronk et al. (2012) and Heister et al. (2012) incubated defined soil components to study the effect of different components on the formation of biogeochemical interfaces and aggregates and, with density fractionation, illustrated that the mineral composite controlled the aggregate structure and that OM was patchily distributed on the specific mineral surface. However, the non-destructive and continuous characterization of the microscale interaction between the soil matrix and microbial processes was still limited by spatial heterogeneity. Our SoilChip method transformed the 3-D structure of soil interfaces into a homogeneous 2-D surface at micro scale (800 μm-diameter), which is excellent for undisturbed measurements and dynamic tracking of BGI development. The SoilChip method is a new technique for studying processes among all original soil components (i.e., soil particles, OM, and microorganisms) at soil BGIs under standardized conditions. Notably, this method includes PDMS surfaces in the soil microenvironment system. Although PDMS is a biocompatible material, its hydrophobic nature could affect the distribution of soil components by attracting hydrophobic substances, including phospholipids. Therefore, PDMS might affect the relative transformation of
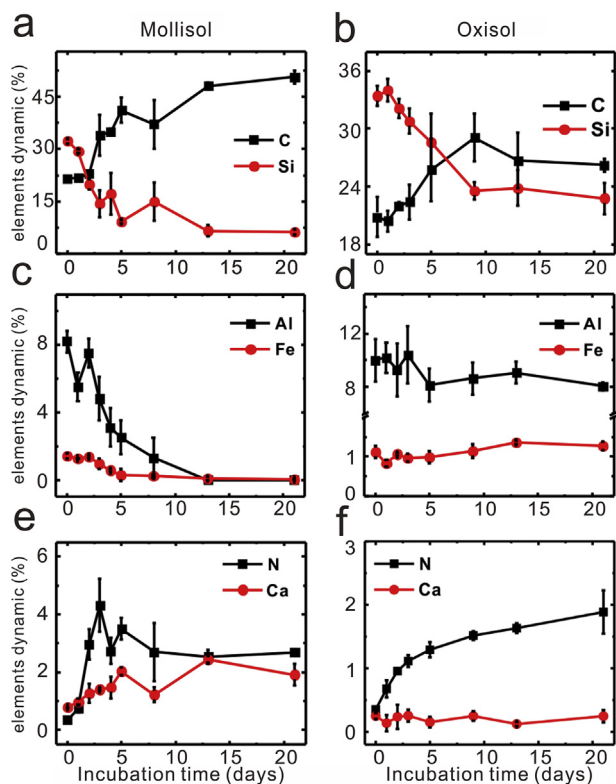
Fig. 5. Dynamics of the main elements (mass concentration >0.5%) at two typical soil biogeochemical interfaces, during a 21-d incubation. Dynamics of C and Si (a and b), Al and Fe (c and d), and N and Ca (e and f) in a Mollisol and an Oxisol, respectively.

substances related to hydrophilic and hydrophobic soil properties on chips and should be studied further.

4.2. Undisturbed monitoring of microbial processes on SoilChips

Microbial processes affect the formation of BGIs (Totsche et al., 2010; Malik et al., 2012; Lamparter et al., 2014) and drive the elemental biogeochemical cycles (Falkowski et al., 2008), whereby microbial growth and metabolism are the basic components of BGI formation in soils. Our results indicate that soil-microbe complexes emerged on the BGIs after 13 d of incubation (Fig. 4a and c). Considering that the DOM added contained no microbial biomass, since it was filtered through a 0.25-μm membrane, we conclude that the microbes on the SoilChips gradually recovered and adapted to the new surroundings, thus enabling them to form soil-microbe complexes. Taking advantage of the continuous evolution of the soil-microbe complexes on the SoilChip, the undisturbed monitoring of the C/N ratio dynamic by XPS illustrates the impact of microbial metabolites on the OM within the BGI.

4.3. Mechanisms of BGI formation

Formation of BGIs was discussed in previous studies (Pronk et al., 2012; Lamparter et al., 2014; Siebecker et al., 2014), indicating that both the physical-chemical and biological properties, such as the solute composition, OM, and biological activities, affected the BGI formation. However, detailed knowledge regarding the interplay and interdependencies of the physical, chemical, and biological processes at the specific BGI remain scarce (Young and Crawford, 2004; Totsche et al., 2010; Schmidt et al., 2011). Our results indicated that the formation features of the BGIs of the two

soils were quite different, such as their microbial communities (Fig. 4) and mineral-organic interactions (Fig. 5), which indicates that the interactions between microorganisms, OM, clay minerals, and Fe/Al-oxides were different as well.

The loss of water during the incubation of the Mollisol enriched the solute concentrations, thereby contributing to an increase in substances, including DOM and bacteria, deposited on the mineral surface (Fig. 5a and c). These concentration processes were also reflected by the gradual accumulation of Ca at the Mollisol BGI (Fig. 5e), which suggests that water loss plays an important role in the composition of the BGI. In addition, considering the increase in microbial biomass (Fig. 4a) and decrease in N at the Mollisol's BGI (Fig. 5e) at the end of the incubation, we suggest that the supply of nutrients and fresh OM sources to the soil microarrays is a decisive factor in triggering microbial processes and regulating the formation of specific BGIs. The OC concentration of the aqueous solution extracted from the Mollisol was greater than that of the Oxisol (111.8 mg/kg vs. 30.6 mg/kg; Table S1). Furthermore, the C 1s spectrum of DOM from the two soils (Fig. S4) revealed that the Oxisol yielded a higher alcoholic carbon than the Mollisol. In combination with the higher C/N ratio of the Oxisol-derived DOM than that of the Mollisol-derived DOM (36 vs. 17); this indicates that the DOM solution from the Oxisol contained more polysaccharide-like substances, whereas the DOM solution extracted from the Mollisol was richer in organic N. Therefore, at the Mollisol BGI, the higher concentration of N (and possibly other nutrients) may have contributed to the greater microbial growth and enhanced metabolic processes, when compared to that of the Oxisol BGI (Fig. 4a and c), thus contributing to the stronger shift of the BGI from predominantly inorganic to predominantly organic. This hypothesis is supported by the dynamics of organic N at the BGIs (Fig. 5e and f), which indicated the occurrence of rapid N assimilation by microbial processes in the Mollisol, being triggered by the N-rich DOM. After the microbial immobilization of N, the microbial community could secrete polysaccharide-rich EPS for further nutrient acquisition and modification of the environment, thus contributing to an increasing C/N ratio (Ye et al., 2011; Chen et al., 2014). This is further supported by the fact that the alcoholic carbon increased with incubation time (data not shown), whereas the total N decreased after 5 days incubation (Fig. 5e), thus suggesting the accumulation of C-O species, such as polysaccharides. Accordingly, the richer nutrient supply at the Mollisol BGI directly enhanced the microbial activity and, consequently, fostered ecological functions, such as a higher OM accumulation (Fig. 5a and b; Zhou et al., 2012; Malik et al., 2013).

In addition to nutrient supply and microbial community in the solution, the mineral composition of the soils also contributed to the accumulation of OM at the BGI (Torn et al., 1997; Kögel-Knabner et al., 2008; Doetterl et al., 2015). The XRD data of clay minerals (Table S5) demonstrated that a greater amount of active components (i.e., montmorillonite, vermiculite, and illite) was present in the clay mineral assemblage of the Mollisol (86%) than in that of the Oxisol (54%), which was richer in the low-activity clay kaolinite, as was also indicated by the bulk soil mineral analysis (Fig. S5). Together with the smaller size distribution of the dispersed Mollisol, when compared to that of the Oxisol (Fig. S1), the mineral surfaces of the Mollisol also provided more active sites for microbe-mediated OM adsorption, thus enhancing the accumulation of OM at its BGIs. However, our dynamic survey of Mollisol BGI revealed a relatively more pronounced depletion in Fe and Al than in Si (Fig. S6). This suggests that OM was preferentially sorbed to the active surfaces of Fe and Al oxides/hydroxides, over those of phyllosilicates, thus corroborating previous studies that clay minerals and iron oxide contribute to the OM sequestration (Kleber et al., 2007; Cao et al., 2011; Vogel et al., 2014).

In the Oxisol, we found that fewer Si and Al surfaces were coated by C, which could have resulted from lower contents of active clay minerals (Table S5). But the percentage of surficial Fe in the Oxisol barely changed during the incubation, compared to the Fe in the Mollisol (Fig. 5c and d; Fig. S6). Considering the OC concentration (Table S1) and composition of DOM (Fig. S4) added to the SoilChip, we suggest that in the Oxisol much less OC and N was available to support microbial growth and metabolism than in the Mollisol, which resulted in the reduced formation of microbial biomass and accumulation of metabolites at the Oxisol BGI. This is supported by the less diverse microbe shapes and sizes (Fig. 4a and c) and lower N accumulation (Fig. 5f) at the Oxisol BGI during the 21 days incubation.

5. Conclusions

To the best of our knowledge, the present study provides the first report of a controllable, living platform for mimicking the microscale processes of soil. By coupling the SoilChip with XPS, we tracked the dynamics of multi-element interactions at soil BGIs. Through the comparative analysis of the formation processes of BGIs in two typical soils of different mineralogical composition, we confirmed that soil BGIs are hotspots for element cycling and are affected by the geochemical background (mineralogical and chemical composition), nutrient supply, and microbial community of the soil. The revived microbial community could be different to the native soil, however, this method provides a model for elucidating the detailed information of the interactions between minerals, OM, and microbes at the BGI, which is meaningful for clarifying the complex mechanisms of the "black box" that controls the biogeochemical cycling of soil. For more insightful investigations of microbe-mediated processes at the soil BGI, staining, isotope tracing, and imaging techniques, such as NanoSIMS, of the SoilChips will be necessary.

Acknowledgments

Appendix A. Supplementary data

Supplementary data related to this article can be found at http://dx.doi.org/10.1016/j.soilbio.2017.05.021.

References

Amelung, W., Kaiser, K., Kammerer, G., Sauer, G., 2002. Organic carbon at soil particle surfaces—evidence from x-ray photoelectron spectroscopy and surface abrasion. Soil Science Society of America Journal 66, 1526—1530.

Arnarson, T.S., Keil, R.G., 2001. Organic—mineral interactions in marine sediments studied using density fractionation and X-ray photoelectron spectroscopy. Organic Geochemistry 32, 1401—1415.

Cai, P., Huang, Q., Walker, S.L., 2013. Deposition and survival of Escherichia coli O157:H7 on clay minerals in a parallel plate flow system. Environmental Science and Technology 47, 1896—1903.

Cao, Y., Wei, X., Cai, P., Huang, Q., Rong, X., Liang, W., 2011. Preferential adsorption of extracellular polymeric substances from bacteria on clay minerals and iron oxide. Colloids and Surfaces B: Biointerfaces 83, 122—127.

Chastain, J., King, R.C., Moulder, J., 1995. Handbook of X-ray Photoelectron Spectroscopy: a Reference Book of Standard Spectra for Identification and Interpretation of XPS Data. Physical Electronics Eden Prairie, MN.

Chen, R., Senbayram, M., Blagodatsky, S., Myachina, O., Dittert, K., Lin, X., Blagodatskaya, E., Kuzyakov, Y., 2014. Soil C and N availability determine the priming effect: microbial N mining and stoichiometric decomposition theories. Globle Change Biology 20, 2356—2367.

Chen, Z., Hou, H., Zheng, Y., Qin, H., Zhu, Y., Wu, J., Wei, W., 2012. Influence of fertilisation regimes on a nosZ-containing denitrifying community in a rice paddy soil. Journal of the Science of Food and Agriculture 92, 1064—1072.

Chorover, J., Kretzschmar, R., Garcia-Pichel, F., Sparks, D.L., 2007. Soil biogeochemical processes within the critical zone. Elements 3, 321—326.

Doetterl, S., Stevens, A., Six, J., Merckx, R., Van Oost, K., Pinto, M.C., Casanova-Katny, A., Muñoz, C., Boudin, M., Venegas, E.Z., 2015. Soil carbon storage controlled by interactions between geochemistry and climate. Nature Geoscience 8, 780—783.

Falkowski, P.G., Fenchel, T., Delong, E.F., 2008. The microbial engines that drive Earth's biogeochemical cycles. Science 320, 1034—1039.

Gleixner, G., 2013. Soil organic matter dynamics: a biological perspective derived from the use of compound-specific isotopes studies. Ecological Research 28, 683—695.

Goebel, M.-O., Bachmann, J., Reichstein, M., Janssens, I.A., Guggenberger, G., 2011. Soil water repellency and its implications for organic matter decomposition - is there a link to extreme climatic events? Global Change Biology 17, 2640—2656.

Grossmann, G., Guo, W.J., Ehrhardt, D.W., Frommer, W.B., Sit, R.V., Quake, S.R., Meier, M., 2011. The RootChip: an integrated microfluidic chip for plant science. Plant Cell 23, 4234—4240.

Heister, K., Höschen, C., Pronk, G.J., Mueller, C.W., Kögel-Knabner, I., 2012. NanoSIMS as a tool for characterizing soil model compounds and organomineral associations in artificial soils. Journal of Soils and Sediments 12, 35—47.

Huang, P.-M., Wang, M.-K., Chiu, C.-Y., 2005. Soil mineral—organic matter—microbe interactions: impacts on biogeochemical processes and biodiversity in soils. Pedobiologia 49, 609—635.

Jozefaciuk, G., Czachor, H., 2014. Impact of organic matter, iron oxides, alumina, silica and drying on mechanical and water stability of artificial soil aggregates. Assessment of new method to study water stability. Geoderma 221, 1—10.

Kögel-Knabner, I., Guggenberger, G., Kleber, M., Kandeler, E., Kalbitz, K., Scheu, S., Eusterhues, K., Leinweber, P., 2008. Organo-mineral associations in temperate soils: integrating biology, mineralogy, and organic matter chemistry. Journal of Plant Nutrition and Soil Science 171, 61—82.

Kaiser, K., Eusterhues, K., Rumpel, C., Guggenberger, G., Kögel-Knabner, I., 2002. Stabilization of organic matter by soil minerals—investigations of density and particle-size fractions from two acid forest soils. Journal of Plant Nutrition and Soil Science 165, 451—459.

Kim, H.J., Boedicker, J.Q., Choi, J.W., Ismagilov, R.F., 2008. Defined spatial structure stabilizes a synthetic multispecies bacterial community. Proceedings of the Nationa Academy of Sciences U S A 105, 18188—18193.

Kleber, M., Eusterhues, K., Keiluweit, M., Mikutta, C., Mikutta, R., Nico, P.S., 2015. Chapter one-mineral—organic associations: formation, properties, and relevance in soil environments. Advances in Agronomy 130, 1—140.

Kleber, M., Sollins, P., Sutton, R., 2007. A conceptual model of organo-mineral interactions in soils: self-assembly of organic molecular fragments into zonal structures on mineral surfaces. Biogeochemistry 85, 9—24.

Kuzyakov, Y., Blagodatskaya, E., Blagodatsky, S., 2009. Comments on the paper by Kemmitt et al. (2008) 'Mineralization of native soil organic matter is not regulated by the size, activity or composition of the soil microbial biomass — a new perspective' [Soil Biology & Biochemistry 40, 61—73]: the biology of the regulatory gate. Soil Biology and Biochemistry 41, 435—439.

Lamparter, A., Bachmann, J., Woche, S.K., Goebel, M.-O., 2014. Biogeochemical interface formation: wettability affected by organic matter sorption and microbial activity. Vadose Zone Journal 13, 0.

Lehmann, J., Kleber, M., 2015. The contentious nature of soil organic matter. Nature 528, 60—68.

Lehmann, J., Solomon, D., Kinyangi, J., Dathe, L., Wirick, S., Jacobsen, C., 2008. Spatial complexity of soil organic matter forms at nanometre scales. Nature Geoscience 1, 238—242.

Li, J., Zhao, B., Li, X., Hwat, B.S., 2008. Effects of long-term combined application of organic and mineral fertilizers on soil microbiological properties and soil fertility. Scientia Agricultura Sinica 41, 144—152.

Li, Y., Chen, P., Wang, Y., Yan, S., Feng, X., Du, W., Koehler, S.A., Demirci, U., Liu, B.F., 2016. Rapid assembly of heterogeneous 3D cell microenvironments in a microgel array. Advanced Materials 28, 3543—3548.

Lützow, M.V., Kogel-Knabner, I., Ekschmitt, K., Matzner, E., Guggenberger, G., Marschner, B., Flessa, H., 2006. Stabilization of organic matter in temperate soils: mechanisms and their relevance under different soil conditions - a review. European Journal of Soil Science 57, 426—445.

Malik, A., Blagodatskaya, E., Gleixner, G., 2013. Soil microbial carbon turnover decreases with increasing molecular size. Soil Biology and Biochemistry 62, 115—118.

Malik, A., Scheibe, A., LokaBharathi, P.A., Gleixner, G., 2012. Online stable isotope analysis of dissolved organic carbon size classes using size exclusion chromatography coupled to an isotope ratio mass spectrometer. Environmental Science and Technology 46, 10123—10129.

McClain, M.E., Boyer, E.W., Dent, C.L., Gergel, S.E., Grimm, N.B., Groffman, P.M., Hart, S.C., Harvey, J.W., Johnston, C.A., Mayorga, E., 2003. Biogeochemical hot spots and hot moments at the interface of terrestrial and aquatic ecosystems. Ecosystems 6, 301–312.

Mikutta, R., Schaumann, G.E., Gildemeister, D., Bonneville, S., Kramer, M.G., Chorover, J., Chadwick, O.A., Guggenberger, G., 2009. Biogeochemistry of mineral–organic associations across a long-term mineralogical soil gradient (0.3–4100kyr), Hawaiian Islands. Geochimica et Cosmochimica Acta 73, 2034–2060.

Mueller, C.W., Weber, P.K., Kilburn, M.R., Hoeschen, C., Kleber, M., Pett-Ridge, J., 2013. Advances in the analysis of biogeochemical interfaces: NanoSIMS to investigate soil microenvironments. Advances in Agronomy 121, 1–46.

O'Donnell, A.G., Young, I.M., Rushton, S.P., Shirley, M.D., Crawford, J.W., 2007. Visualization, modelling and prediction in soil microbiology. Nature Review Microbiology 5, 689–699.

Oades, J., Waters, A., 1991. Aggregate hierarchy in soils. Soil Research 29, 815–828.

Pronk, G.J., Heister, K., Ding, G.-C., Smalla, K., Kögel-Knabner, I., 2012. Development of biogeochemical interfaces in an artificial soil incubation experiment; aggregation and formation of organo-mineral associations. Geoderma 189, 585–594.

Remusat, L., Hatton, P.J., Nico, P.S., Zeller, B., Kleber, M., Derrien, D., 2012. NanoSIMS study of organic matter associated with soil aggregates: advantages, limitations, and combination with STXM. Environmental Science and Technology 46, 3943–3949.

Sapsford, K.E., Ligler, F.S., 2004. Real-time analysis of protein adsorption to a variety of thin films. Biosensors and Bioelectronics 19, 1045–1055.

Schmidt, M.W., Torn, M.S., Abiven, S., Dittmar, T., Guggenberger, G., Janssens, I.A., Kleber, M., Kogel-Knabner, I., Lehmann, J., Manning, D.A., Nannipieri, P., Rasse, D.P., Weiner, S., Trumbore, S.E., 2011. Persistence of soil organic matter as an ecosystem property. Nature 478, 49–56.

Siebecker, M., Li, W., Khalid, S., Sparks, D., 2014. Real-time QEXAFS spectroscopy measures rapid precipitate formation at the mineral-water interface. Nature Communication 5, 5003.

Six, J., Bossuyt, H., Degryze, S., Denef, K., 2004. A history of research on the link between (micro) aggregates, soil biota, and soil organic matter dynamics. Soil and Tillage Research 79, 7–31.

Sparks, D.L., 2015. Advances in coupling of kinetics and molecular scale tools to shed light on soil biogeochemical processes. Plant and Soil 387, 1–19.

Torn, M.S., Trumbore, S.E., Chadwick, O.A., Vitousek, P.M., Hendricks, D.M., 1997. Mineral control of soil organic carbon storage and turnover. Nature 389, 170–173.

Totsche, K.U., Rennert, T., Gerzabek, M.H., Kögel-Knabner, I., Smalla, K., Spiteller, M., Vogel, H.-J., 2010. Biogeochemical interfaces in soil: the interdisciplinary challenge for soil science. Journal of Plant Nutrition and Soil Science 173, 88–99.

Valiei, A., Kumar, A., Mukherjee, P.P., Liu, Y., Thundat, T., 2012. A web of streamers: biofilm formation in a porous microfluidic device. Lab on a Chip 12, 5133–5137.

Vogel, C., Mueller, C.W., Hoschen, C., Buegger, F., Heister, K., Schulz, S., Schloter, M., Kogel-Knabner, I., 2014. Submicron structures provide preferential spots for carbon and nitrogen sequestration in soils. Nature Communication 5, 2947.

Wan, J., Tyliszczak, T., Tokunaga, T.K., 2007. Organic carbon distribution, speciation, and elemental correlations within soil microaggregates: applications of STXM and NEXAFS spectroscopy. Geochimica et Cosmochimica Acta 71, 5439–5449.

Weibel, D.B., Diluzio, W.R., Whitesides, G.M., 2007. Microfabrication meets microbiology. Nature Review Microbiology 5, 209–218.

Wessel, A.K., Hmelo, L., Parsek, M.R., Whiteley, M., 2013. Going local: technologies for exploring bacterial microenvironments. Nature Review Microbiology 11, 337–348.

Woche, S.K., Goebel, M.-O., Mikutta, R., Schurig, C., Kaestner, M., Guggenberger, G., Bachmann, J., 2017. Soil wettability can be explained by the chemical composition of particle interfaces – an XPS study. Scientific Reports 7, 42877.

Ye, F., Ye, Y., Li, Y., 2011. Effect of C/N ratio on extracellular polymeric substances (EPS) and physicochemical properties of activated sludge flocs. Journal of Hazardous Materials 188, 37–43.

Young, I.M., Crawford, J.W., 2004. Interactions and self-organization in the soil-microbe complex. Science 304, 1634–1637.

Yuan, G., Soma, M., Seyama, H., Theng, B., Lavkulich, L., Takamatsu, T., 1998. Assessing the surface composition of soil particles from some Podzolic soils by X-ray photoelectron spectroscopy. Geoderma 86, 169–181.

Zhou, J., Xue, K., Xie, J., Deng, Y., Wu, L., Cheng, X., Fei, S., Deng, S., He, Z., Van Nostrand, J.D., 2012. Microbial mediation of carbon-cycle feedbacks to climate warming. Nature Climate Change 2, 106–110.